

A Novel Supramolecular Assembly Film of Porphyrin Bound DNA: Characterization and Catalytic Behaviors Towards Nitric Oxide

Jianping Lei ¹, Huangxian Ju ² and Osamu Ikeda ^{1,*}

¹ Department of Chemistry, Faculty of Science, Kanazawa University, Natural Science Hall 1, Kakuma, Kanazawa, Ishikawa 920-1192, Japan

² State Key Laboratory of Coordination Chemistry, Department of Chemistry, Institute of Chemical Biology, Nanjing University, Nanjing 210093, P.R. China

*Author to whom correspondence should be addressed. E-mail: osamu@kenroku.kanazawa-u.ac.jp

Received: 28 May 2004 / Accepted: 29 September 2004 / Published: 26 April 2005

Abstract: A stable Fe(4-TMPyP)-DNA-PADDA (FePyDP) film was characterized on pyrolytic graphite electrode (PGE) or an indium-tin oxide (ITO) electrode through the supramolecular interaction between water-soluble iron porphyrin (Fe(4-TMPyP)) and DNA template, where PADDA (poly(acrylamide-*co*-diallyldimethylammonium chloride) is employed as a co-immobilizing polymer. Cyclic voltammetry of FePyDP film showed a pair of reversible Fe^{III}/Fe^{II} redox peaks and an irreversible Fe^{IV}/Fe^{III} peak at -0.13 V and +0.89 vs. Ag|AgCl in pH 7.4 PBS, respectively. An excellent catalytic reduction of NO was displayed at -0.61 V vs. Ag|AgCl at a FePyDP film modified electrode. Chronoamperometric experiments demonstrated a rapid response to the reduction of NO with a linear range from 0.1 to 90 μ M and a detection limit of 30 nM at a signal-to-noise ratio of 3. On the other hand, it is the first time to apply high-valent iron porphyrin as catalyst at modified electrode for NO catalytic oxidation at +0.89 vs. Ag|AgCl. The sensor shows a high selectivity of some endogenous electroactive substances in biological systems. The mechanism of response of the sensors to NO is preliminary studied.

Keywords: nitric oxide determination, supramolecular assembly, porphyrin bound DNA, Electrochemical sensor.

Introduction

Since Malinski and Taha [1] reported the application of an electropolymerized nickel porphyrin film electrode for the detection of NO, the metalloporphyrin biosensor has intensively been investigated for amperometric measurements of NO [2-8]. The methods for the immobilization of metalloporphyrins onto the electrode surface include electropolymerization of metalloporphyrins [2-3], doping with metalloporphyrins of polypyrrole film [4-5], and deposition of metalloporphyrins entrapped in Nafion film [6-8]. In order to obtain better analytical performance of the electrochemical NO sensors, it is a significant goal to develop new materials for modifying porphyrin on electrode surfaces.

DNA is of considerable interest due to their potential applications as biological materials and probes for nucleic acid structure and dynamics. DNA film has been used as an electroconductive biological film [9,10]. Giese et al. [9] suggested a multistep hopping mechanism for the long distance charge migration along the double-strand of DNA. Okahata et al. [10] directly observed the switchable electron conduction along intramolecular DNA strands by using DNA-lipid cast film on a comb-type electrode. Immobilized DNA on an electrode can act as a DNA sensor.

The binding of porphyrin with DNA is presumably stabilized by electrostatic interaction between the positively charged substituent on the porphyrin periphery and the negatively charged phosphate group of DNA. Three major modes have been proposed for the binding of cationic porphyrins with DNA: intercalation, outside binding without self-stacking, and outside binding with self-stacking along the nucleic acids surface [11-12]. The supramolecular interaction and direct electron transfer between cationic porphyrins and their derivatives with DNA on the electrode has been served as a model system for the understanding of electron transfer mechanisms in biological systems [13].

Iron(III) meso-tetrakis(*N*-methylpyridinium-4-yl)porphyrin (Fe(4-TMPyP)) is the water-soluble porphyrin with positive charges at the peripheries. Circular dichroism spectrum and UV-vis spectrum suggested the interaction between positively charged Fe(4-TMPyP) and the negatively charged DNA template form a stable complex of DNA-bound-porphyrin with the ratio of the molar ratio of 1:5 Fe(4-TMPyP):DNA phosphate [11, 14]. Also, our previous research has demonstrated that the reaction of Fe(4-TMPyP) with NO undergoes a reductive nitrosylation in a wide pH range [15] and the selective catalytic oxidation of NO can be performed against nitrite by iron(IV) porphyrin at an ITO electrode in aqueous solutions [16,17].

In this study, we prepared a novel porphyrin film, Fe(4-TMPyP)-DNA-PADDA (FePyDP) film, through the supramolecular assembly of cationic porphyrins into DNA template and developed a new NO sensor. The mechanisms of catalysis of NO have been proposed on a FePyDP film modified electrode.

Experimental

Chemicals

Fe^{III}(4-TMPyP) was prepared according to the methods suggested by Pasternack et al. [18] and Bedioui et al. [19]. The product was purified by chromatography with help of anion exchange resin. Salmon testis double strand (ST-ds) DNA (Sigma), and poly(acrylamide-*co*-diallyldimethylammonium chloride) (PADDA, Aldrich) were used as received. DNA concentration was estimated in nucleotide phosphate, which was determined using spectrophotometer with ϵ of $1.31 \times 10^4 \text{ M}^{-1} \text{ cm}^{-1}$ at 260 nm [11].

All solutions were deoxygenated by bubbling ultrapure argon gas (Nippon Sanso, 99.9999%) for 20 min. NO-saturated solution was prepared by bubbling mixed gas of 5% NO and 95% Ar (Nippon Sanso) for 30 min into a deoxygenated solution before each electrochemical and spectroscopic run. The NO gas mixture was purified from possible traces of high-valent nitrogen oxides and dioxygen by passing through three successive vials containing a 10% solution of potassium hydroxide, an alkaline solution of pyrogallol, and pure water finally. The molar concentration of NO in solution was evaluated from Ostwald's solubility coefficient [20] for a given partial pressure of NO. All aqueous solutions were prepared with twice distilled water.

Preparation of DNA-PADDA composite and cast films

The mixture of 0.3 mL aqueous solution of 15 mg mL^{-1} ST-dsDNA and 0.2 mL aqueous solution of 15 mg mL^{-1} PADDA was set at a room temperature for 30 min until a white precipitate of DNA-PADDA was formed. After being set at ambient temperature overnight, the solution was centrifuged, and the sediment was washed with pure water and then dried at a room temperature. Such dried DNA-PADDA composite powder was dispersed in water by ultrasonication for 30 min to obtain a DNA-PADDA cloudy suspension of 3 mg mL^{-1} . Prior to casting, the suspension was ultrasonicated for another 10 min.

Edge plane PGE was abraded with metallographic sandpaper (2000 grit) and then polished on a clean billiard cloths with $0.06 \mu\text{m}$ aluminum powder for about 3 min, followed by ultrasonication in pure water for 2 min. $10 \mu\text{L}$ 3 mg mL^{-1} DNA-PADDA suspension was cast on the cleaned electrode surface and dried in air overnight. After the electrode was soaked in water for at least 4 h and rinsed with water to remove any unadsorbed composite, one DNA-PADDA film modified PGE was obtained. The electrode was then immersed in $2 \times 10^{-4} \text{ M}$ Fe(4-TMPyP) solution for 60 min to prepare Fe(4-TMPyP)-DNA-PADDA (FePyDP) film. A similar process was applied to indium tin oxide (ITO) transparent electrode for UV-vis spectroscopy (Hitachi U2000).

Electrochemical apparatus

Electrochemical data were collected with an electrochemical workstation (BAS, model 100B/W) in one three-electrode cell protected against air penetration. The working areas of an optically transparent ITO electrode and a PG electrode were 18.2 mm² and 7.1 mm², respectively. The Ag | AgCl | 3 M NaCl electrode (BAS, RE-5) and a platinum coil were utilized as reference and counter electrodes, respectively.

Quartz crystal microbalance (QCM) measurements

The assembly process was monitored on a QCA917 type quartz crystal microbalance (SEIKO EG&G Co., Japan) linked to a personal computer for the microgravimetric analysis. QCM crystals used for the quantification of immobilized Fe(4-TMPyP) were at 9 MHz. An AT-cut shear mode quartz crystal deposited gold on both sides with a geometric area of 0.2 cm² was used. A typical QCM experiment began from the cleaning of the Au/quartz crystal surface with a piranha solution (30% H₂O₂ and 70% concentrated H₂SO₄). After rinsing with twice-distilled water, the Au/quartz crystal was dried over a stream of N₂ gas. Following the same procedure as on PGE, a DNA-PADDA modified Au/quartz crystal electrode was prepared. The Au/quartz crystal electrode was sealed in an electrolytic cell with a Teflon casing, and one side was exposed to 2×10⁻⁴ M Fe(4-TMPyP) solution for *in-situ* frequency measurements.

Results and Discussion

Preparation and characterization of FePyDP film-modified electrode

Figure 1A shows the electrochemical response of DNA-PADDA film on the PGE in 2×10⁻⁴ M Fe(4-TMPyP) PBS (pH 7.4), performed by consecutive cyclic voltammetry between potentials of -0.4 and +0.5 V. As can be seen, the growth of the cyclic voltammogram current in Fig. 1 shows an Fe^{III}/Fe^{II} redox couple of Fe(4-TMPyP) with a formal potential, E° , of -0.13 V vs. Ag|AgCl, which was slightly higher than that determined in the same pH solution on bare PGE.

This electrochemical result is consistent with the QCM data (Fig. 1B). On a bare Au/quartz crystal electrode, no significant frequency change was observed on the QCM electrode. However, the DNA-PADDA modified Au/crystal electrode showed an obvious frequency decrease. The change was attributed to the entrapping of Fe(4-TMPyP) in DNA-PADDA film. In the first stage, a sharp decrease of the frequency was observed. The first-order rate constant was obtained by curve fitting as a characteristic time of immobilization, τ , of 15 min. The immobilization rate constant was 34 ng min⁻¹. The total change in the frequency corresponded to an accumulation of 0.65 μ g in the film after interaction with Fe(4-TMPyP) for 60 min toward a saturation value.

Electronic absorption spectrum of the FePyDP-modified ITO transparent electrode showed a red shift in the Soret band from 422 nm to 428 nm and a new absorption peak appeared at 515 nm, comparing with the spectrum of free Fe(4-TMPyP) in solution (Table 1). Obviously, DNA-bound-porphyrin was formed by assembly of Fe(4-TMPyP) in DNA-PADDA film. A theoretical study has clarified that a thermodynamically stable DNA-bound-porphyrin was formed through π - π stacking interaction in the DNA minor groove [21]. The corresponding binding constants were calculated to be $(3.7 \pm 0.5) \times 10^5 \text{ M}^{-1}$ by spectroscopic titration [14].

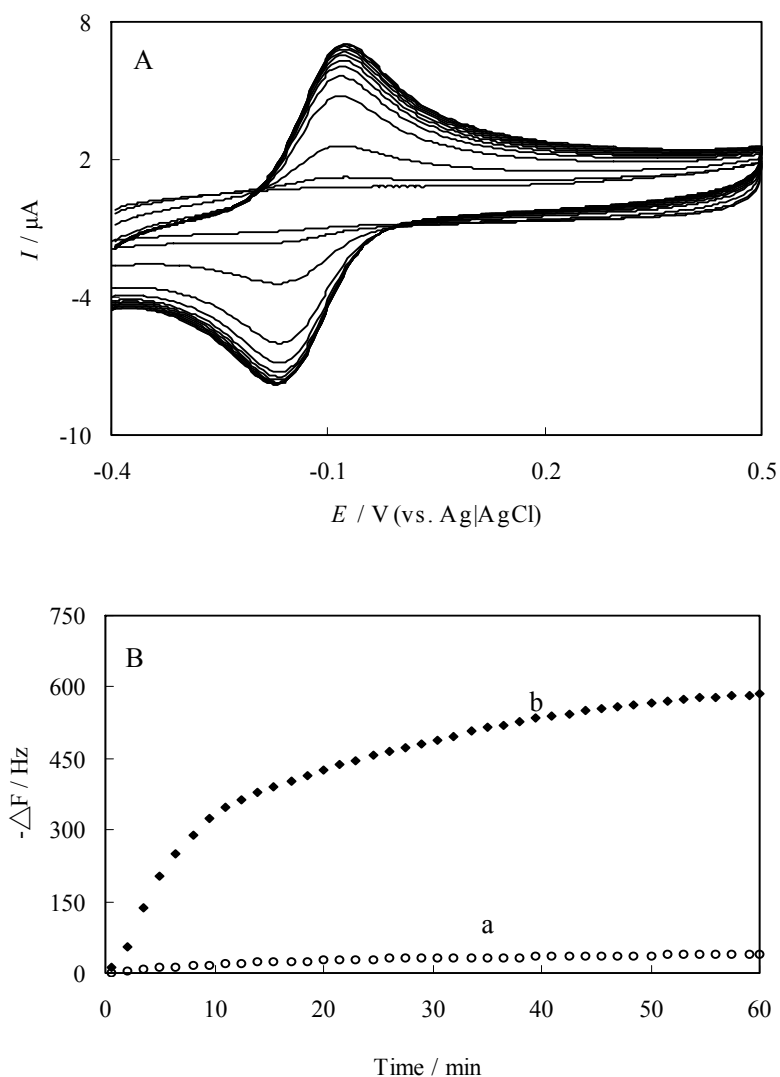


Figure 1. (A) Cyclic voltammograms of DNA-PADDA film in a 0.05 M PBS (pH 7.4) containing $2 \times 10^{-4} \text{ M}$ Fe(4-TMPyP) obtained at different soaking times (each 5 minutes) from inner to outside. Scan rate, 200 mV s^{-1} . (B) *In-situ* monitoring of the frequency decreases ($-\Delta F$) with the time for the immobilization of $2 \times 10^{-4} \text{ M}$ Fe(4-TMPyP) in pH 7.4 PBS onto (a) a bare Au/quartz crystal, and (b) a DNA-PADDA modified Au/quartz crystal electrode.

Table 1. Spectrophotometric characteristics of Fe(4-TMPyP) in various systems.

Porphyrin complexes	UV-Vis spectroscopy	
	Soret band λ (nm)	Q bands λ (nm)
FePyDP film on ITO in PBS (pH 7.4)	428	515
Fe(4-TMPyP) solution in PBS (pH 7.4) ^a	422	490, 598
FePyDP film on ITO in the presence of saturated NO	425	557

^a Absorption spectrum of 1×10^{-4} M Fe(4-TMPyP) solution was obtained in an optically transparent thin layer cell which was composed of two ITO-coated glass plates with the optical pathlength of ca. 0.2 mm.

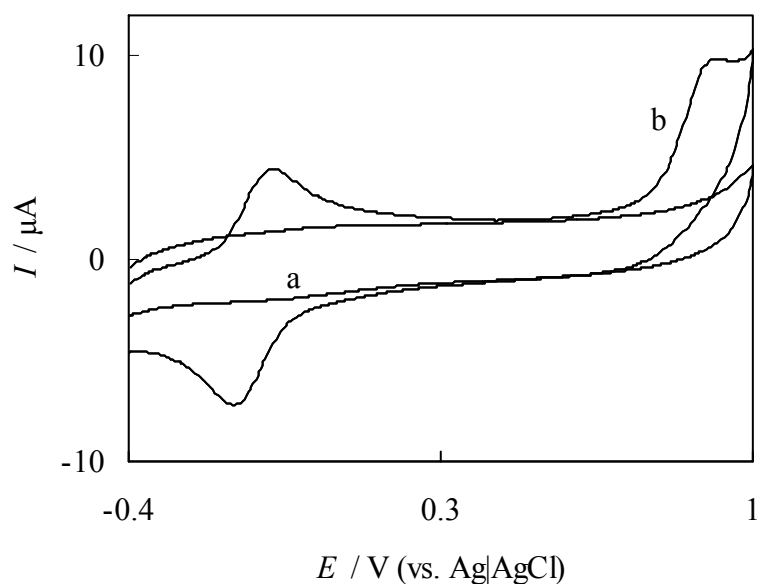


Figure 2. Cyclic voltammograms of DNA-PADDA film in a 0.05 M PBS (pH 7.4) (a) before and (b) after soaking 60 minutes. Scan rate, 200 mV s^{-1}

Fig. 2 is the cyclic voltammogram obtained at a FePyDP and DNA-PADDA film-modified electrode in pH 7.4 PBS. The FePyDP film modified electrode showed a couple of characteristic $\text{Fe}^{\text{III}}/\text{Fe}^{\text{II}}$ redox peaks of Fe(4-TMPyP) at -0.10 V and -0.17 V for a sweep rate of 200 mV s^{-1} with the peak-to-peak separation (ΔE_p) of ca. 72 mV (Fig. 2b). In contrast, no CV peak was observed at the DNA-PADDA film-modified electrode under the same conditions in this potential range (Fig. 2a).

These results suggested a direct electron transfer between Fe(4-TMPyP) and the electrode. An irreversible oxidation wave with peak potential about +0.89 V vs. Ag|AgCl, corresponding to the Fe^{IV}/Fe^{III} redox potential, occurs at a more positive potential than the Fe^{III}/Fe^{II} redox couple. Spectroelectrochemistry identified this oxidation current occurs from the transfer to an oxoiron(IV) species, which has the typical double peaks in the visible region of an oxoiron(IV) (Fe^{IV}=O) group by applying potential of +0.9 V vs. Ag|AgCl [17].

Catalytic reduction of NO at FePyDP film-modified PG electrode

In our previous works, it has been reported a reductive nitrosylation as a probable pathway to explain the observed phenomenon in solution [15]. We propose a similar reduction process of Fe(III) with NO at a FePyDP film electrode, as following:



This reductive nitrosylation has been described for a number of heme proteins and model complexes [22]. Absorption spectrum also suggested a strong interaction between Fe(4-TMPyP) and NO when NO was added to the electrochemical cell. The absorption spectrum of Fe^{III}(4-TMPyP) in FePyDP film in pH 7.4 PBS showed a Soret band at 428 nm. After bubbling 5% NO gas up to saturation in this solution, however, it was observed that the λ_{max} value was blue-shifted from 428 nm to 425 nm (Table 1). Such a blue shift at the Soret band is known to be a characteristic of NO binding to iron(II) porphyrins [15]. Therefore, this result suggested that the reaction was thermodynamically favorable to form Fe^{II}(NO)(4-TMPyP). Fe^{II}(NO)(4-TMPyP) was stable for the reduction or oxidation in the potential range of -0.6 +0.35 V vs. Ag|AgCl.

At the DNA-PADDA film modified electrode the voltammogram of NO in pH 7.4 PBS showed a small current at -0.90 V (Fig. 3c). A large reductive current was observed in the presence of NO at the FePyDP film modified electrode, while the redox peaks of Fe(4-TMPyP) disappeared (Fig. 3a). Comparing with the DNA/hemoglobin film [23,24], the catalytic reduction potential of NO on the FePyDP film was positively shifted from -0.68V to -0.61V vs. Ag|AgCl. The large reductive current resulted from the catalytic reduction of NO by the immobilized Fe(4-TMPyP), and peak current ratio was ca. 15 for the peak current vs. the noncatalytic Fe^{III/II} reduction peak at the saturation concentration of 100 % NO (1.8 mM). The above results indicated a high catalytic activity of iron porphyrin for NO reduction at FePyDP film-modified electrode. More interestingly, an addition of nitrite into pure Fe(4-TMPyP) solution caused little change in the cyclic voltammogram (Figs. 2b and 3b). This indicated that nitrite could not be reduced at the FePyDP film-modified electrode in this potential range. As a conclusion, it was clarified that the FePyDP film exhibited a selective catalytic reduction of NO against NO₂⁻.

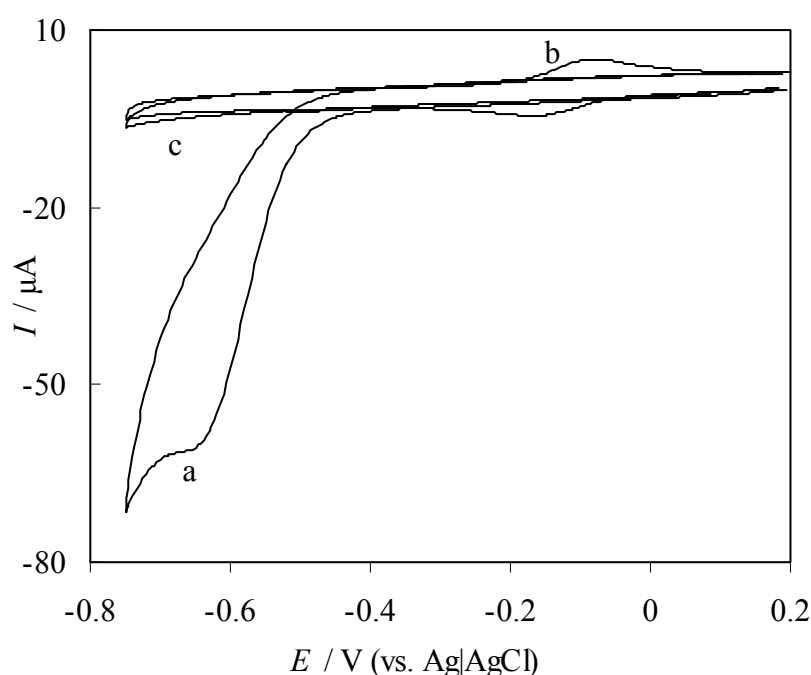
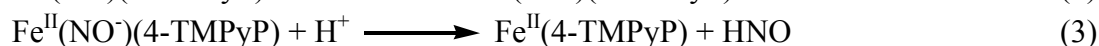


Figure 3. Cyclic voltammograms of FePyDP film modified PG electrode in 50 mM PBS (pH 7.4) (a) with 82.3 μM NO and (b) with 100 μM NO_2^- . Curve (c) is obtained in pure PBS at DNA-PADDA film with 82.3 μM NO. Scan rate, 200 mV s^{-1} .

To obtain more detailed analysis, cyclic voltammetry was carried out at different pH values. As increasing the pH, the catalytic peak currents ($I_{\text{cat,p}}$) decreased and the catalytic peak potentials shifted to more negative potentials, which indicated proton accelerated the reduction of NO at the FePyDP film-modified electrode. As discussed above, the catalytic current corresponded to the reduction of ferrous-nitrosyl adduct, $\text{Fe}^{\text{II}}(\text{NO})\text{TMPyP}$, to produce a nitroxyl intermediate (Eq. (2)).



Such a reduction of $\text{Fe}^{\text{II}}\text{-NO}$ nitrosyl adduct to give a nitroxyl intermediate has been previously reported in the case of MbFe incorporated in DDAB film [25]. It was clear that $\text{Fe}^{\text{II}}(\text{NO}^-)(4\text{-TMPyP})$ was unstable and was irreversibly transformed into the ferrous form by a nucleophilic attack of proton [26]. The dissociation of $\text{Fe}^{\text{II}}(\text{NO}^-)(4\text{-TMPyP})$ was promoted at low pH, leading to the increase of a catalytic current with decreasing pH. The pH dependence of the catalytic current suggested that the nitroxyl immediate could be decomposed by the loss of HNO, which then rapidly coupled in solution to form N_2O (Eq. (4)).



This result supports a CEC mechanism as shown in Eqs 1, 2 and 3. In a conclusion, the FePyDP film electrode displayed excellent catalytic activity for the NO reduction at -0.61 V vs. Ag|AgCl. The whole reduction process of NO was a typical CEC mechanism.

Quantification of NO using the proposed FePyDP modified electrode was carried out by a chronoamperometry at -700 mV. All measurements were performed with strict exclusion of molecular oxygen, and the electrodes have been conditioned by means of cyclic voltammetry prior to the measurement. The inset in Fig. 4 shows a typical amperometric response with successive additions of NO. The sensor showed a response time of 1.5 s after NO addition, indicating a fast response to NO reduction. The calibration curve of the sensor showed a linear response in the NO concentration range of 1.0×10^{-7} to 9.0×10^{-5} M with a correlation coefficient of 0.9987 (Fig. 4). From the slope of $0.049 \mu\text{A } \mu\text{M}^{-1}$, the detection limit calculated at a signal-to-noise ratio of 3 was 3.0×10^{-8} M.

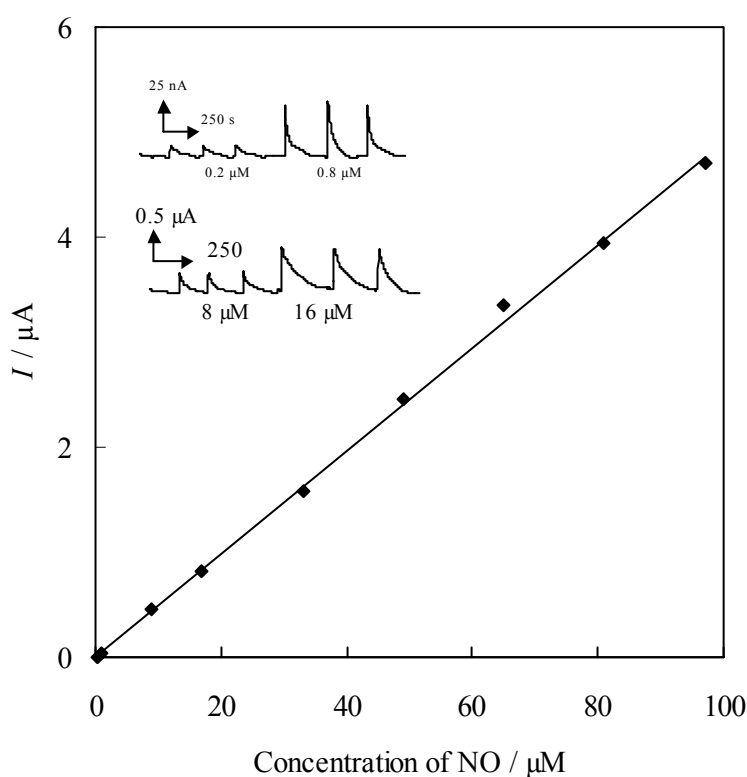


Figure 4. Calibration curve for amperometric determination of NO at a FePyDP modified PGE. Applied potential, -700 mV vs. (Ag|AgCl). Inset: amperometric response upon injection of NO solution.

Since the estimated amount of NO released from the single cell is about 1-200 attomol, i.e. 2×10^{-4} - 1×10^{-6} M, the detection limit of the proposed sensor would be suitable for in vivo determination of NO. The stability of the sensor was good. It was used for at least two weeks without an obvious decrease in

the response to NO, when the sensors were kept in a phosphate buffer solution with pH 7.4 at 4°C. Reproducibility as the NO sensor at different electrodes (n=11) was investigated by injections of 8 µM NO. The relative standard deviation (RSD) of catalytic current was 6.3%. It was clarified that this FePyDP film modified electrode showed a good reproducibility for the response of NO.

Catalytic oxidation of NO at FePyDP film modified ITO electrode

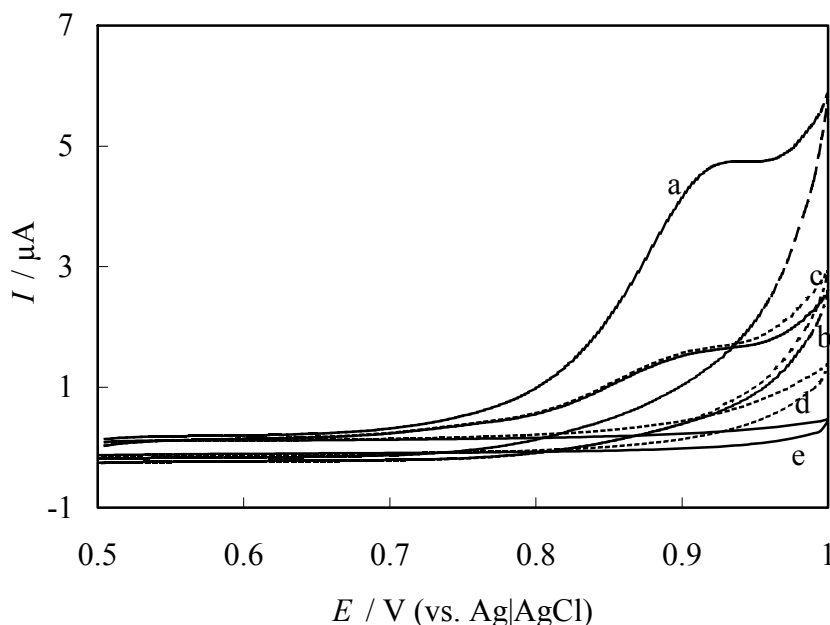
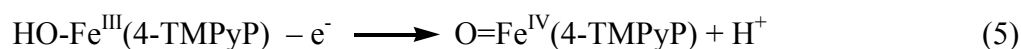


Figure 5. Cyclic voltammograms of FePyDP film modified ITO electrode in 50 mM PBS (pH 7.4) (a) with and (b) without 82.3 µM NO, and (c) with 100 µM NO₂⁻. Curves (d) and (e) are obtained in pure PBS at DNA-PADDA film with and without 82.3 µM NO. Scan rate, 10 mV s⁻¹.

Figure 5 shows cyclic voltammograms of NO at a FePyDP film modified electrode in 50 mM, pH 7.4 PBS. The direct oxidation of NO at the DNA-PADDA film modified ITO electrode (Fig. 5d) was observed with a quite small current in the potential region below 1.0 V, which is more positive than the formation potential of Fe(IV) porphyrin at ITO. However, the presence of Fe^{III}(4-TMPyP) (Fig. 5a) resulted in a significant current increase. A comparison of Fig. 5a with Fig. 5b indicates that the oxidation of NO proceeds along with the oxidation of Fe^{III}(4-TMPyP). These results suggested one catalytic process of Fe^{III}(4-TMPyP) towards the NO oxidation through an EC catalytic regeneration mechanism. A feature of this mechanism was that the iron porphyrin must firstly be oxidized to O=Fe^{IV}(4-TMPyP) at a FePyDP film modified electrode as shown in the following equations [17].



To our knowledge, it was the first report on the application of oxoiron(IV) porphyrin as a catalyst at modified electrode for catalytic oxidation of NO.

Comparing with Fig. 5b and 5c, an addition of nitrite into the PBS solution caused little change of the cyclic voltammogram in the potential window of +0.5 to +1.0 V at the FePyDP film modified ITO electrode. The electrochemical response obtained in the presence of nitrite was only 1% of that obtained for the NO alone in solution. Thus, nitrite was not oxidized in that potential range. $O=Fe^{IV}(4-TMPyP)$ showed a high selectivity for NO oxidation against NO_2^- . In addition, when both NO and nitrite were present in the solution. The electrocatalytic wave is very similar to that observed in the absence of nitrite. As a conclusion, $O=Fe^{IV}(4-TMPyP)$ selectively oxidized NO to form NO_2^- anion. Herold [27] noted the rapid formation of a $MbFe^{III}ONO$ intermediate in the reaction between $MbFe^{IV}=O$ and NO. The direct incorporation of this oxygen atom into NO, yielding nitrite, may account for the relatively rapid reaction rate via a synchronous process [16]. On the other hand, the CVs for the catalytic oxidation of NO at the FePyDP film modified electrode at various scan rates (10-400 mV/s) were carried out. The peak potential shifted in a positive direction with an increase in the scan rate, eventually very close to the oxidation potential of $Fe^{III}(4-TMPyP)$ itself at a high scan rate. The catalytic peak current $i_{p,cat}$ was directly proportional to the square root of the scan rate ($v^{1/2}$), as expected for a diffusion-controlled reaction.

These above results indicated that the catalytic oxidation cycle of NO by oxoiron (IV) porphyrin was a typical chemical catalysis via an intermediate to give nitrite as the product [28], which led FePyDP film modified ITO electrode can be used in NO determination with low interference of nitrite.

Table 2. Interference from other substance for NO determination

Substance	Concentration (1×10^{-5} M)	Relative peak current
Nitrite	10	101.2
L(+)-Ascorbate	20	102.4
Dopamine	1	98.5
Uric acid	1	104.3
D-cysteine	1	105.6
D(+)-Glucose	20	97.1

The selectivity of this electrode was further considered since various interferences such as ascorbate, uric acid, cysteine, glucose and dopamine co-exist with NO in vivo. CV results show that only 5% decrease or increase is seen and show little interference to NO determination at concentrations 1-2 orders of magnitude higher than that expected in biological systems (Table 2). In a conclusion, FePyDP film modified ITO electrode exhibits the selectivity of this NO biosensor is satisfactory.

Conclusions

In this study, we prepared a novel porphyrin film, Fe(4-TMPyP)-DNA-PADDA (FePyDP) film, through the supramolecular assembly of cationic porphyrins into DNA template and provide new insights on the water-soluble porphyrin modified electrode as third reagentless biosensor. The modified electrode displayed an excellent catalytic activity for NO reduction at -0.61 V vs. Ag|AgCl via a CEC electrocatalytic mechanism and NO oxidation at $+0.89$ vs. Ag|AgCl mediated by oxoiron(IV) porphyrin complexes via a typical chemical catalysis, respectively. The selectively catalyzed behaviors of NO against nitrite, based on supramolecular assembly film, can provide an elegant way to prepare NO sensors with high performance characteristics without a drastic diminution in the analytical response and loss probable sensitivity.

References

1. Malinski, T.; Taha, Z. Nitric oxide release from a single cell measured in situ by a porphyrinic-based microsensor. *Nature* **1992**, *358*, 676.
2. Bedioui, F.; Trevin, S.; Albin, V.; Villegas, M.G.G.; Devynck, J. Design and characterization of chemically modified electrodes with iron(III) porphyrinic-based polymers: Study of their reactivity toward nitrites and nitric oxide in aqueous solution. *Anal. Chim. Acta* **1997**, *341*, 177.
3. Vilakazi, S.L.; Nyokong, T. Electrocatalytic properties of vitamin B₁₂ towards oxidation and reduction of nitric oxide. *Electrochim. Acta* **2000**, *46*, 453.
4. Diab, N.; Schuhmann, W. Electropolymerized manganese porphyrin/polypyrrole films as catalytic surfaces for the oxidation of nitric oxide. *Electrochim. Acta* **2001**, *47*, 265.
5. Ciszewski, A.; Kubaszewski, E.; Lozynski, M. The role of nickel as central metal in conductive polymeric porphyrin film for electrocatalytic oxidation of nitric oxide. *Electroanalysis* **1996**, *8*, 293.
6. Hayon, J.; Ozer, D.; Rishpon, J.; Bettelheim, A. Spectroscopic and electrochemical response to nitrogen monoxide of a cationic iron porphyrin immobilized in nafion-coated electrodes or membranes. *J. Chem. Soc. Chem. Commun.* **1994**, 619.
7. Kashevskii, A.V.; Safronov, A. Y.; Ikeda, O. Behaviors of H₂TPP and CoTPPCl in Nafion film and the catalytic activity for nitric oxide oxidation. *J. Electroanal. Chem.* **2001**, *510*, 86.
8. Kashevskii, A.V. Lei, J.; Safronov, A.Y.; Ikeda, O. Electrocatalytic properties of meso-tetraphenylporphyrin cobalt for nitric oxide oxidation in methanolic solution and in Nafion[®] film. *J. Electroanal. Chem.* **2002**, *531*, 71.
9. Giese, B.; Biland, A. Recent developments of charge injection and charge transfer in DNA. *Chem. Commun.* **2002**, 667.
10. Nakayama, H.; Ohno, H.; Okahata, Y. Intramolecular electron conduction along DNA strands and their temperature dependency in a DNA-aligned cast film. *Chem. Commun.* **2001**, 2300.

11. Pasternack, R.F.; Gibbs, E.J.; Villafranca, J.J. Interactions of porphyrins with nucleic acids. *Biochemistry* **1983**, *22*, 2406.
12. Makundan, N.E.; Petho, G.; Dixon, D.W.; Marzilli, L.G. DNA-tentacle porphyrin interactions: AT over selectivity exhibited by an outside binding self-stacking porphyrin. *Inorg. Chem.* **1995**, *34*, 3677.
13. Bakker, E.; Telting-Diaz, M. Electrochemical sensors. *Anal. Chem.* **2002**, *74*, 2781.
14. Lei, J.P.; Ju, H.X.; Ikeda, O. Supramolecular assembly of porphyrin bound DNA and its catalytic behavior for nitric oxide reduction. *Electrochimica Acta* **2004**, *49*, 2453.
15. Trofimova, N.S.; Safronov, A.Y.; Ikeda, O. Electrochemical and spectral studies on the reductive nitrosylation of water-soluble iron porphyrin. *Inorg. Chem.* **2003**, *42*, 1945.
16. Lei, J.P.; Trofimova, N.S.; Ikeda, O. Selective oxidation of nitric oxide against nitrite by oxo-iron(IV) porphyrin at an ITO electrode. *Chem. Lett.* **2003**, *32*, 610.
17. Lei, J.P.; Ju, H.X.; Ikeda, O. Catalytic oxidation of nitric oxide and nitrite mediated by water-soluble high-valent iron porphyrins at an ITO electrode. *J. Electroanal. Chem.* **2004**, *567*, 331.
18. Pasternack, R.F.; Lee, H.; Makel, P.; Spencer, C. Solution properties of tetrakis-(4-N-methyl) -pyridylporphineiron(III). *J. Inorg. Nucl. Chem.* **1977**, *39*, 1865.
19. Bedioui, F.; Bouhier, Y.; Sorel, C.; Devynck, J.; Coche-Guerente, L.; Deronzier, A.; Moutet, J.C. Incorporation of anionic metalloporphyrins into poly(pyrrole-alkylammonium) film: Characterization of the reactivity of the iron(III) porphyrinic-based polymer. *Electrochim. Acta* **1993**, *38*, 2485.
20. D. R. Lide (Ed.), *CRC Handbook of Chemistry and Physics*, 76 th ed., CRC Press, Boca Raton, FL, **1995**, section 6-3.
21. Borissevitch, I.E.; Gandini, S.C.M. Photophysical studies of excited-state characteristics of meso-tetrakis(4-N-methyl-pyridiniumyl) porphyrin bound to DNA. *J. Photochem. Photobiol. B: Biol.* **1998**, *43*, 112.
22. Hoshino, M.; Maeda, M.; Konishi, R.; Seki, H.; Ford, P.C. Studies on the reaction mechanism for reductive nitrosylation of ferrihemoproteins in buffer solutions. *J. Am. Chem. Soc.* **1996**, *118*, 5702.
23. Fan, C.H.; Li, G.X.; Zhu, J.Q.; Zhu, D.X. A reagentless nitric oxide biosensor based on hemoglobin-DNA films. *Anal. Chim. Acta* **2000**, *423*, 95.
24. Fan, C.H.; Chen, X.C.; Li, G.X.; Zhu, J.Q.; Zhu, D.X.; Scheer, H. Direct electrochemical characterization of the interaction between haemoglobin and nitric oxide. *Phys. Chem. Chem. Phys.* **2000**, *2*, 4409.
25. Bayachou, M.; Lin, R.; Cho, W.; Farmer, P.J. Electrochemical reduction of NO by myoglobin in surfactant film: characterization and reactivity of the nitroxyl (NO⁻) adduct. *J. Am. Chem. Soc.* **1998**, *120*, 9888.
26. Barley, M. H.; Rhodes, M. R.; Meyer, T. J. Electrocatalytic Reduction of Nitrite to Nitrous Oxide and Ammonia Based on the N-Methylated, Cationic Iron Porphyrin Complexes [Fe^{III}(H₂O)(TMP_yP)]⁵⁺. *Inorg. Chem.* **1987**, *26*, 1746.

27. Herold, S.; Rehmann, F.K. Kinetic and mechanistic studies of the reactions of nitrogen monoxide and nitrite with ferryl myoglobin. *J. Bio. Inorg. Chem.* **2001**, *6*, 543.
28. Lexa, D.; Saveant, J.M.; Schafer, H.J.; Su, K.B.; Vering, B.; Wang, D.L. Outer-sphere and inner-sphere processes in reductive elimination. Direct and indirect electrochemical reduction of vicinal dibromoalkanes. *J. Am. Chem. Soc.* **1990**, *112*, 6162.